Supplementary Information: Overshooting the critical threshold for the Greenland ice sheet

Nils Bochow*[1,2], Anna Poltronieri[1], Alexander Robinson[3,4], Martin Rypdal[1], and Niklas Boers[5,6,7]

[1] *Department of Mathematics and Statistics, University of Tromsø, Norway.*

[2] *Physics of Ice, Climate and Earth, Niels Bohr Institute, University of Copenhagen, Denmark.*

[3] *Department of Earth Science and Astrophysics, Complutense University of Madrid, Madrid, Spain*

[4] *Instituto de Geociencias, CSIC-UCM, Madrid, Spain*

[5] *Earth System Modelling, School of Engineering & Design, Technical University of Munich, Germany.*

[6] *Potsdam Institute for Climate Impact Research, Germany.*

[7] *Department of Mathematics and Global Systems Institute, University of Exeter, UK.*

January 20, 2023

The supplementary information contains 19 supplementary figures and 3 supplementary tables.

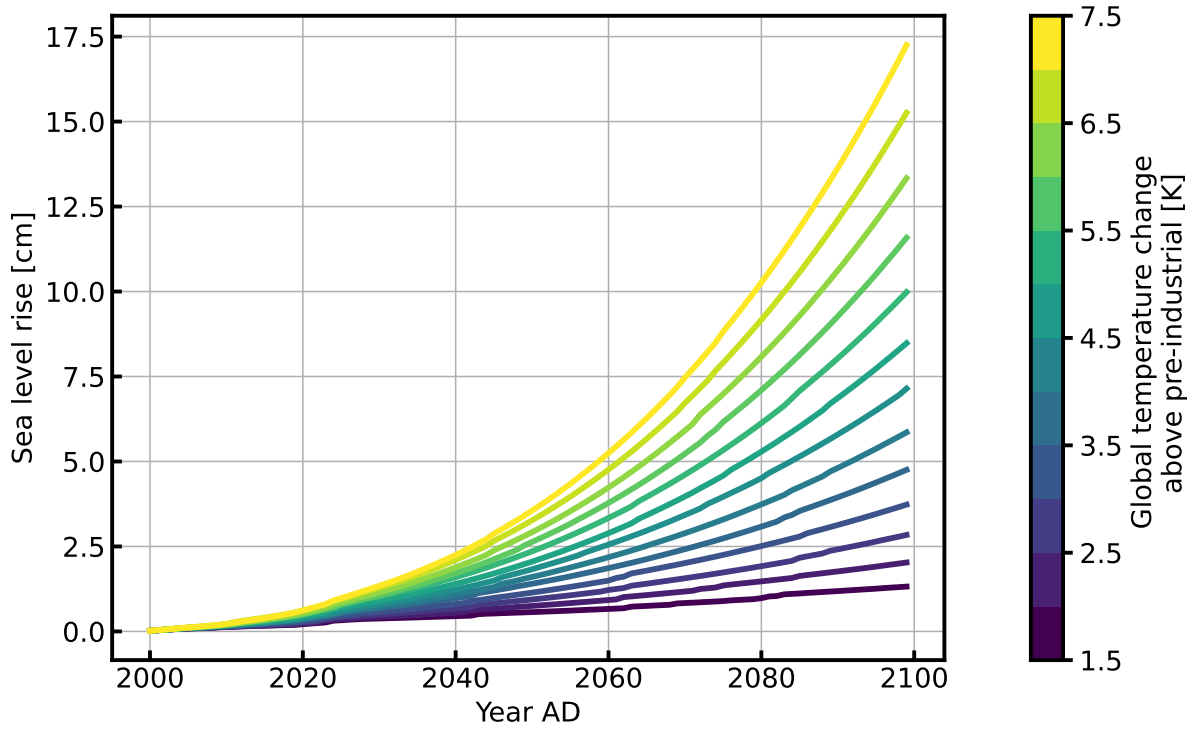

Figure S1: Sea level rise potential of the GrIS for the 21st century for all applied warming scenarios. Sea level rise until the year 2100 for GMT rise between 1.5 °C and 7.5 °C. The sea level rise ranges from 1 cm to 17.5 cm.

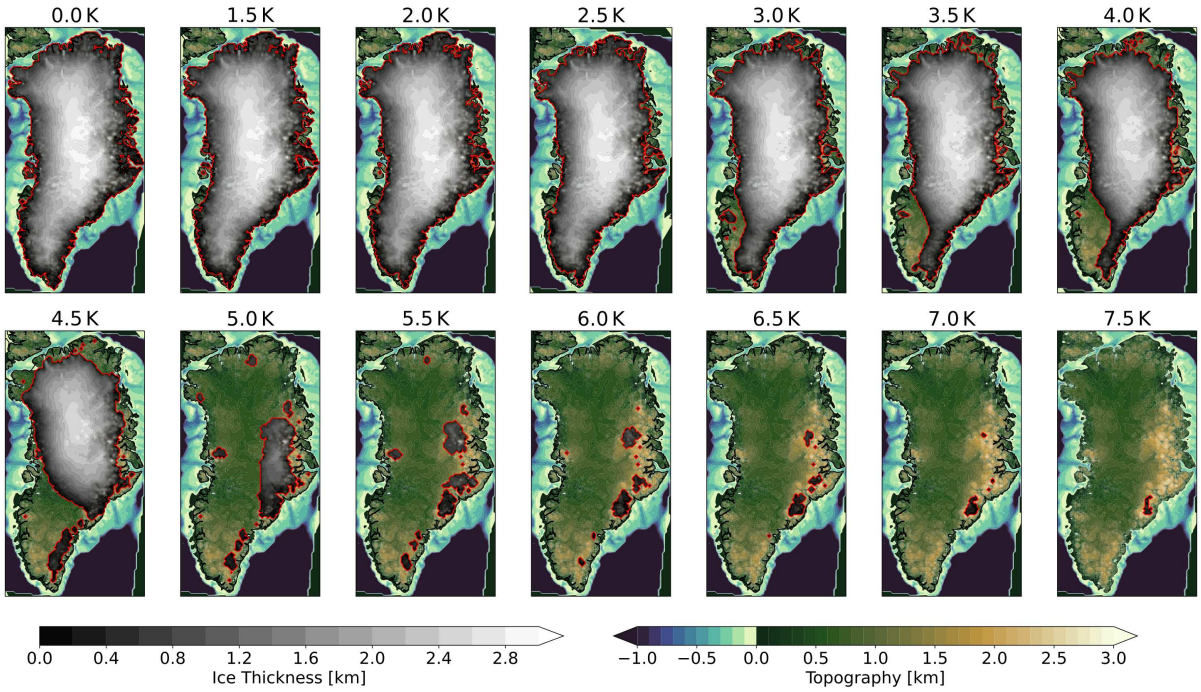

Figure S2: Spatial maps of the GrIS after 100 ka for different warming scenarios. Equilibrium states of the Greenland ice sheet for global warming rates between 0 °C and 7.5 °C. The warming period lasts for 100 years and the temperature is kept constant afterwards. Several different states are distinct: present-day configuration with fully extended ice sheet, several intermediate states with around 50-90% of present-day ice volume for warming rates between 0 °C and 4.5 °C, and an ice free state. The ice sheet extent is denoted by a red outline. The spatial configurations correspond to the end states in Fig. 1.

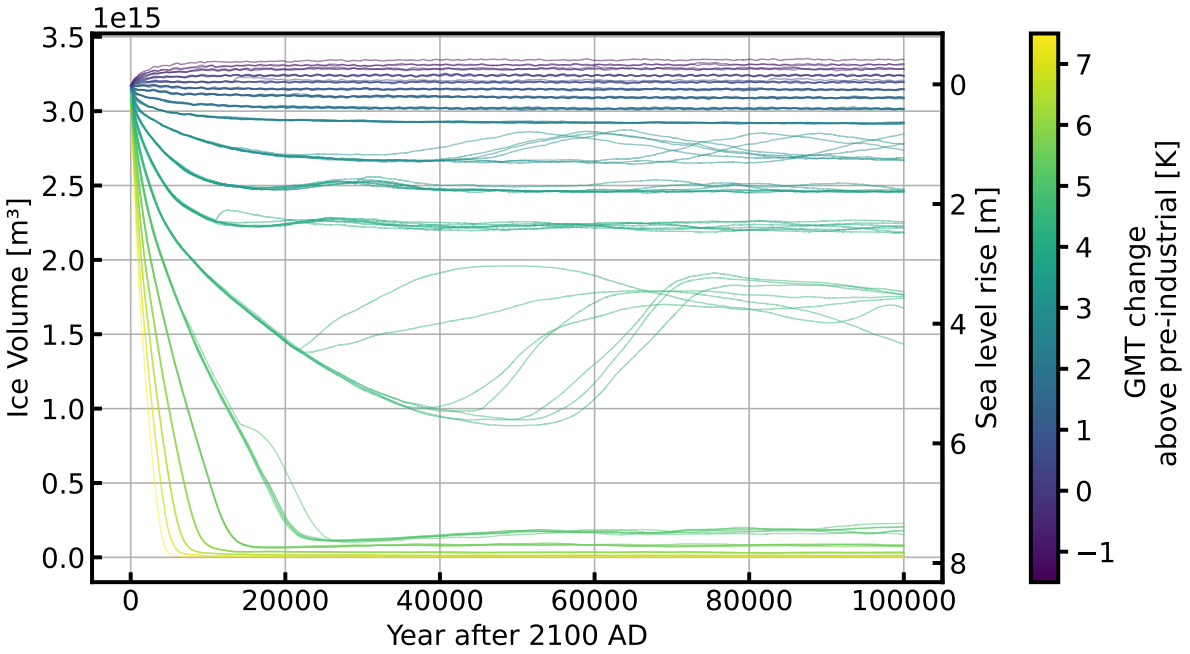

Figure S3: Extended time series of ice volume for different warming scenarios. Evolution of ice volume of whole GrIS for temperature changes between −1.5 °C and 7.5 °C. The warming period lasts for 100 years (1.5 °C to 7.5 °C) with subsequent cooling for another 100 years (−0.5 °C to −3.0 °C). The absolute temperature change is the difference between the warming and cooling. Three different states are distinct: present-day configuration with fully extended ice sheet, intermediate state with around 55% of present-day ice volume, and an ice free state. Temporal extension until the year 100 ka for two runs, representing the evolution of the semi-stable intermediate and the ice-free state. The semi-stable state recovers close to present-day ice sheet volume after 100 ka due to the glacial isostatic adjustment. The single run of the ice-free state shows oscillatory behaviour on the time scale of 10 ka between 10% and 20% of present-day ice volume. The corresponding spatial maps are shown in Fig. 1 and the resulting stability diagram is shown in Fig. 2.

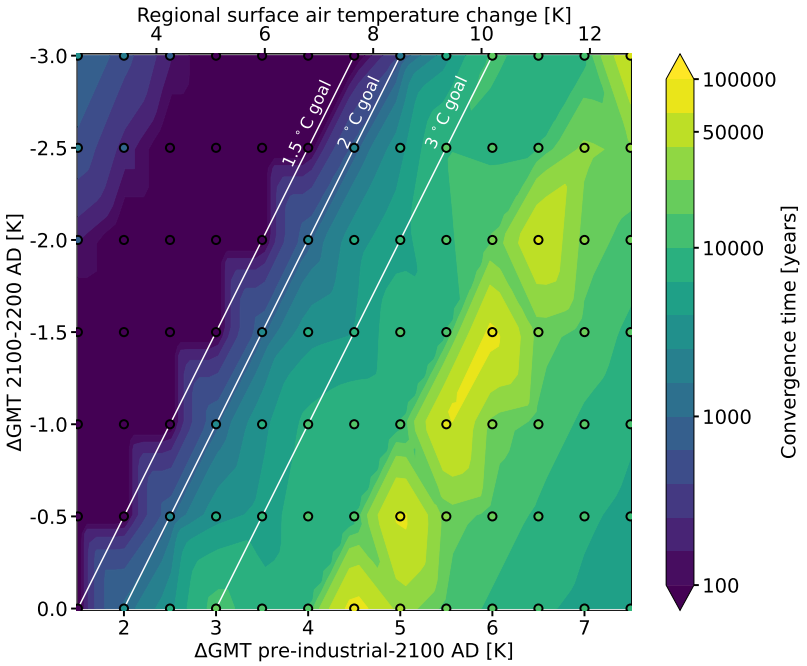

Figure S4: Equilibrium time of the GrIS after warming and subsequent cooling. (a) Equilibrium time for all the considered warming and cooling scenarios. We define the equilibrium time as the first time the ice sheet volume does not exceed a yearly change of more than $1{\cdot}10^{14}\,\mathrm{m}^3$ in 10000 consecutive years. The diagram corresponds to the simulations shown in Fig. 2 and Fig. S3). Different warming rates are applied for 100 years, subsequently we apply various cooling rates for another 100 years. The temperature is kept constant afterwards for another 100 ka. Purple regions denote a short convergence time, the ice sheet does not lose equilibrium for the applied warming and cooling. Green-blue regions reach equilibrium after several millennia to decamillennia, while yellow denotes do not reach a classical equilibrium after 100 ka. We interpolate the stability diagram linearly between the single simulation runs (dots).

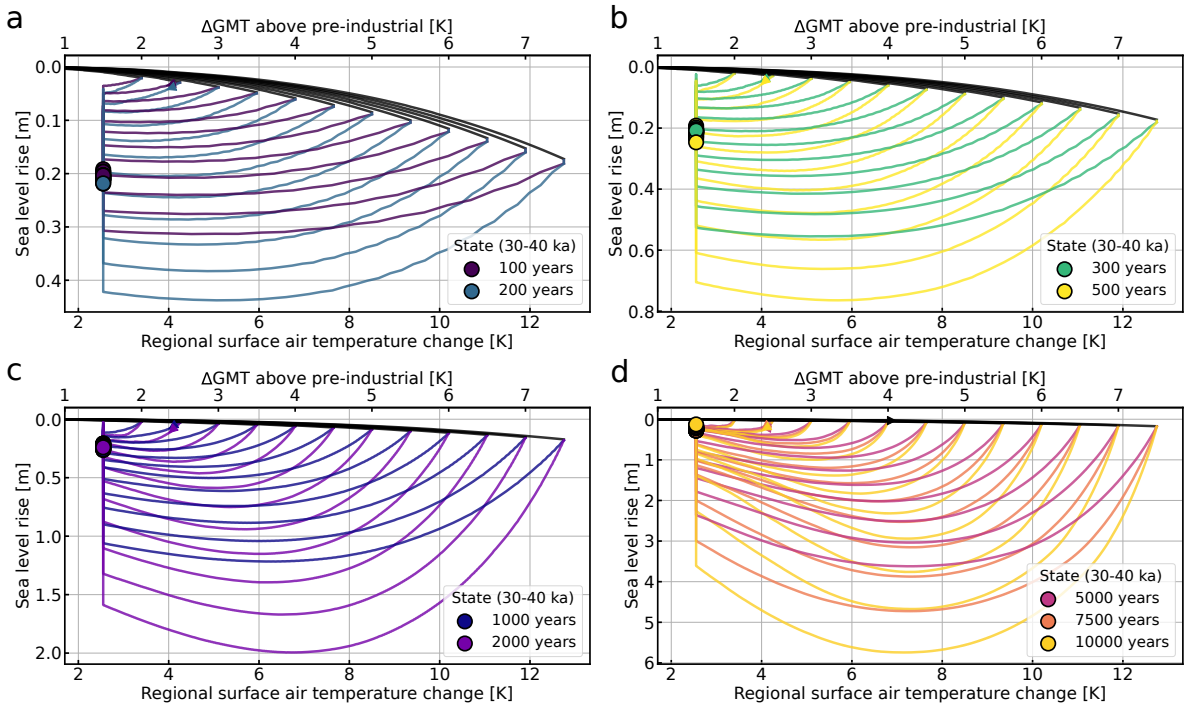

Figure S5: Trajectories of overshoot scenarios for various warming and convergence rates to 1.5 °C. (a) Trajectories of ice sheet volume for various warming rates and subsequent convergence to 1.5 °C GMT above pre-industrial level for 100 and 200 years. The ice sheet recovers to a close to present-day configuration with around 20 cm GSLR. Longer convergence times and larger warming cause larger ice sheet loss before partial recovery. **(b)**, **(c)** and **(d)** same as **(a)** but for convergence times between 300 and 10000 years.

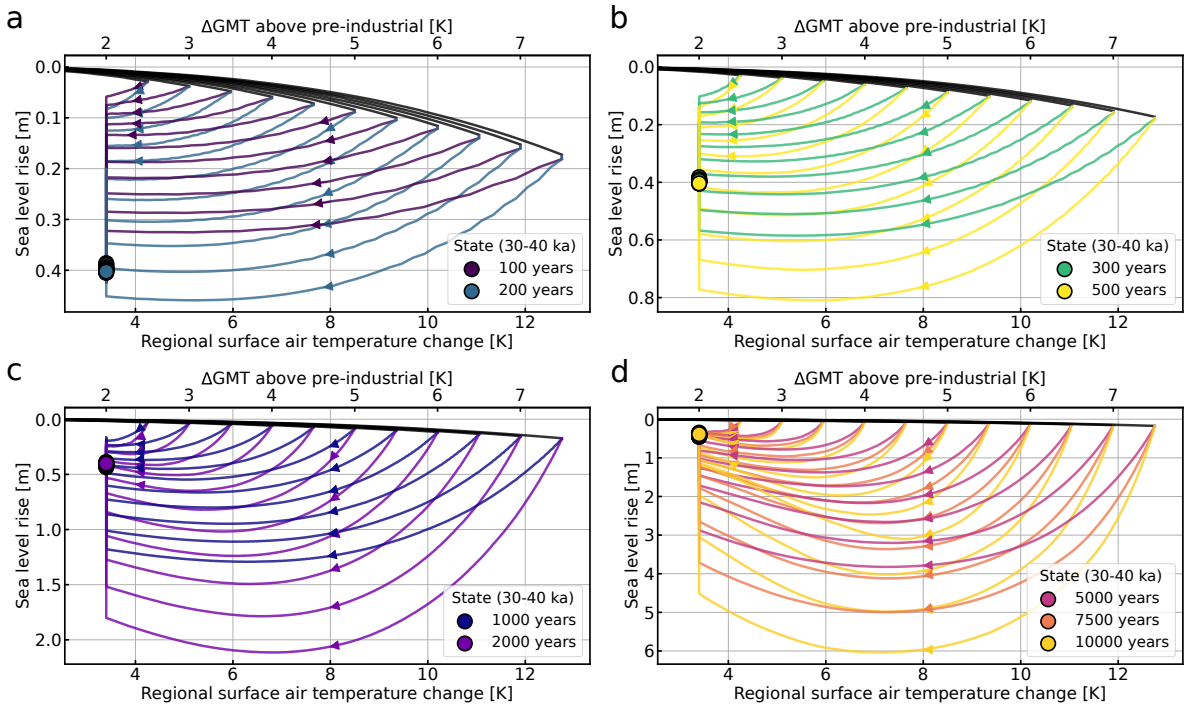

Figure S6: Trajectories of overshoot scenarios for various warming and convergence rates to 2 °C. (a) Trajectories of ice sheet volume for various warming rates and subsequent convergence to 2 °C GMT above pre-industrial level for 100 and 200 years. The ice sheet recovers to a close to present-day configuration with around 40 cm GSLR. Longer convergence times and larger warming cause larger ice sheet loss before partial recovery. **(b)**, **(c)** and **(d)** same as **(a)** but for convergence times between 300 and 10000 years.

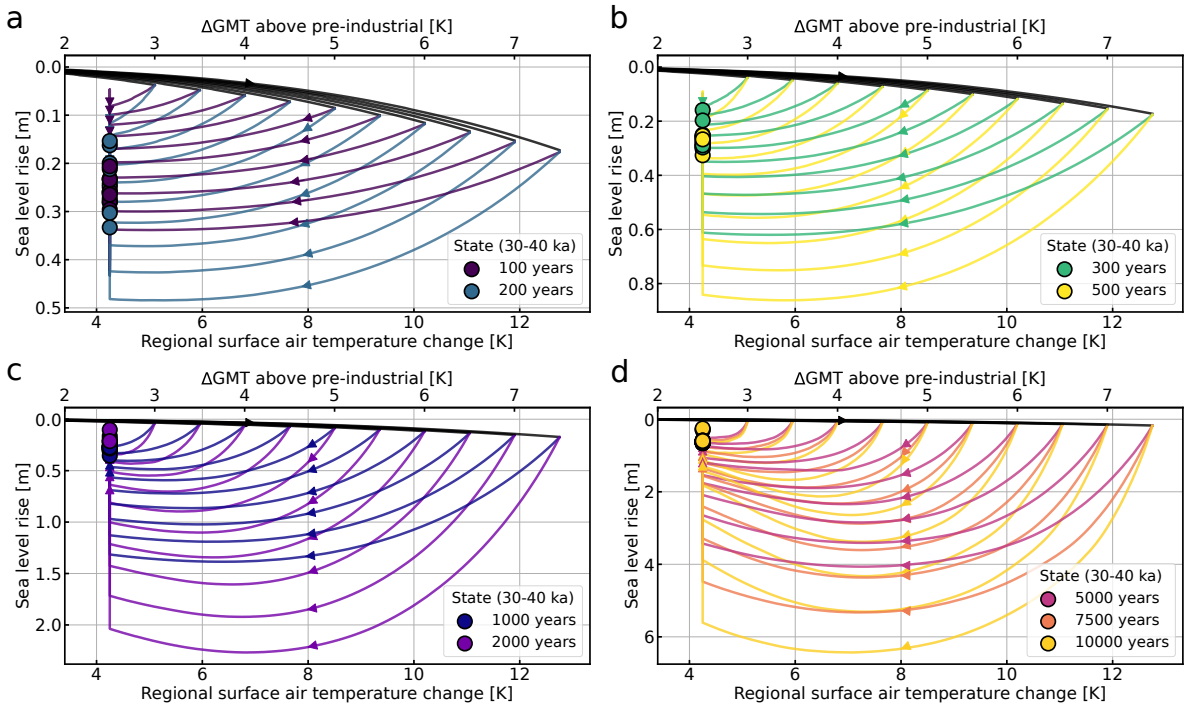

Figure S7: Trajectories of overshoot scenarios for various warming and convergence rates to 2.5 °C. (a) Trajectories of ice sheet volume for various warming rates and subsequent convergence to 2.5 °C GMT above pre-industrial level for 100 and 200 years. The ice sheet recovers to a close to present-day configuration with around 10-40 cm GSLR. Longer convergence times and larger warming cause larger ice sheet loss before partial recovery. **(b)**, **(c)** and **(d)** same as **(a)** but for convergence times between 300 and 10000 years.

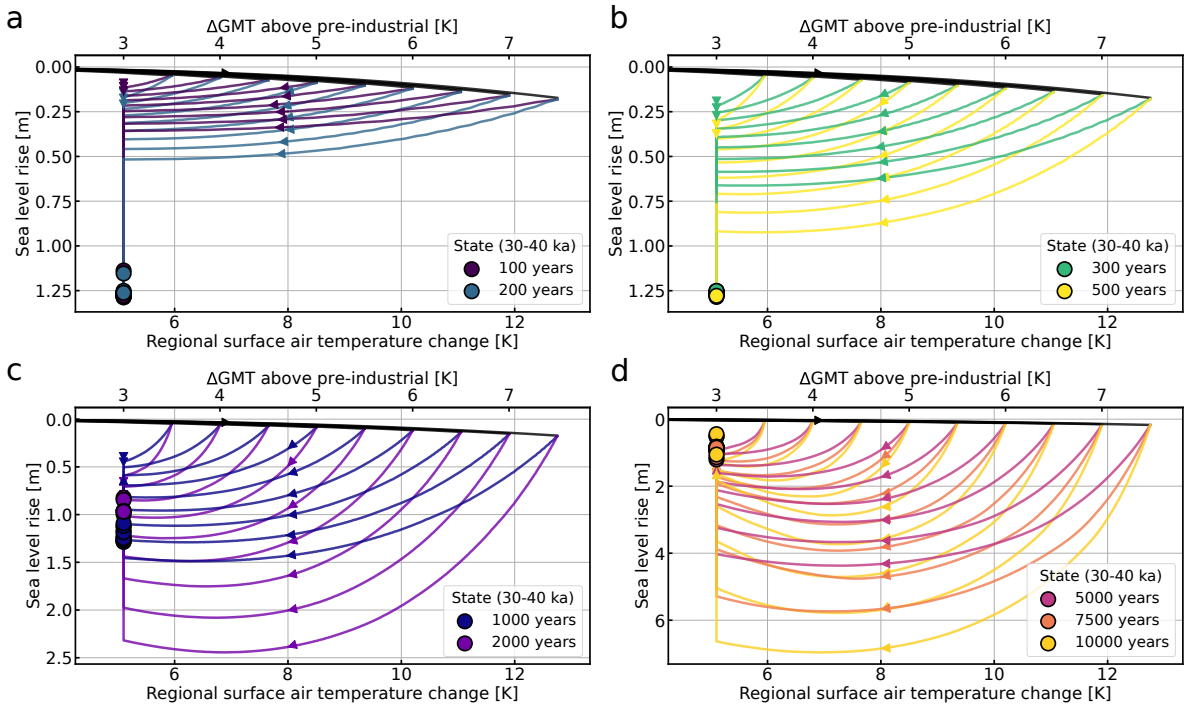

Figure S8: Trajectories of overshoot scenarios for various warming and convergence rates to 3.0 °C. (a) Trajectories of ice sheet volume for various warming rates and subsequent convergence to 3.0 °C GMT above pre-industrial level for 100 and 200 years. The ice sheet recovers to a close to present-day configuration with around 1-1.5 m GSLR. Longer convergence times and larger warming cause larger ice sheet loss before partial recovery. **(b)**, **(c)** and **(d)** same as **(a)** but for convergence times between 300 and 10000 years. The ice volume after 30-40 ka is significantly lower than for more moderate scenarios (Fig. S6).

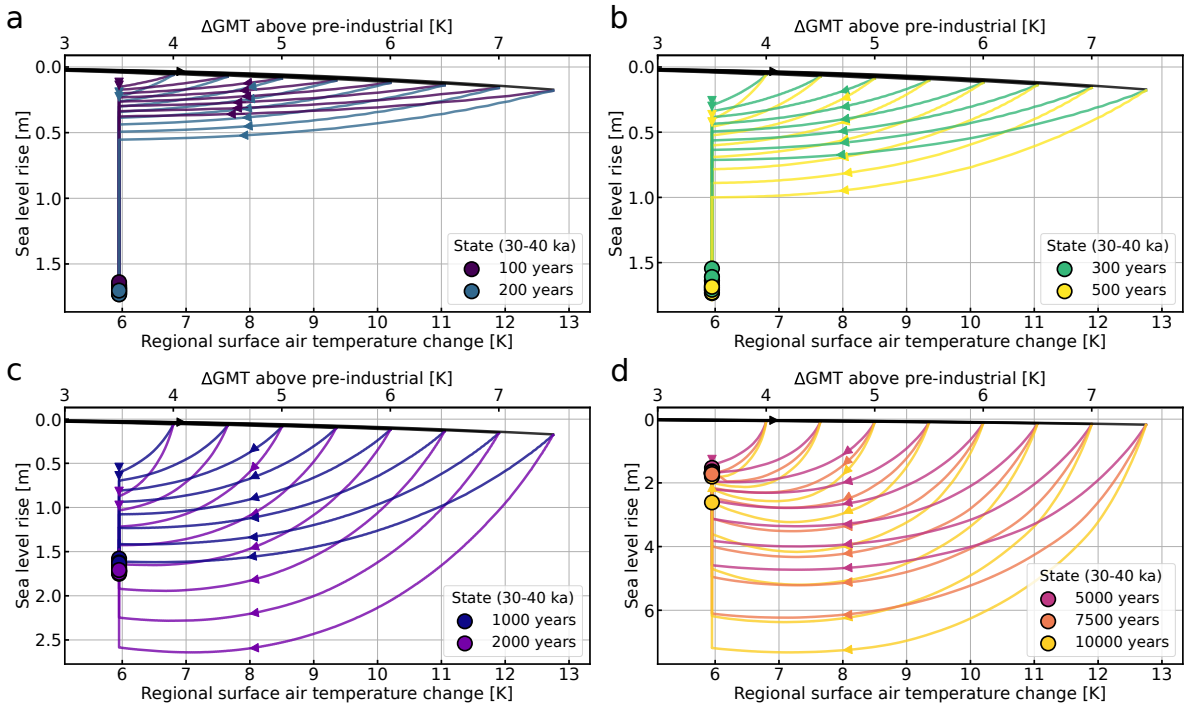

Figure S9: Trajectories of overshoot scenarios for various warming and convergence rates to 3.5 °C. (a) Trajectories of ice sheet volume for various warming rates and subsequent convergence to 3.5 °C GMT above pre-industrial level for 100 and 200 years. The ice sheet recovers to a close to present-day configuration with around 1.5-2.0 m GSLR. Longer convergence times and larger warming cause larger ice sheet loss before partial recovery. **(b)**, **(c)** and **(d)** same as **(a)** but for convergence times between 300 and 10000 years. The ice volume after 30-40 ka is significantly lower than for more moderate scenarios (Fig. S6).

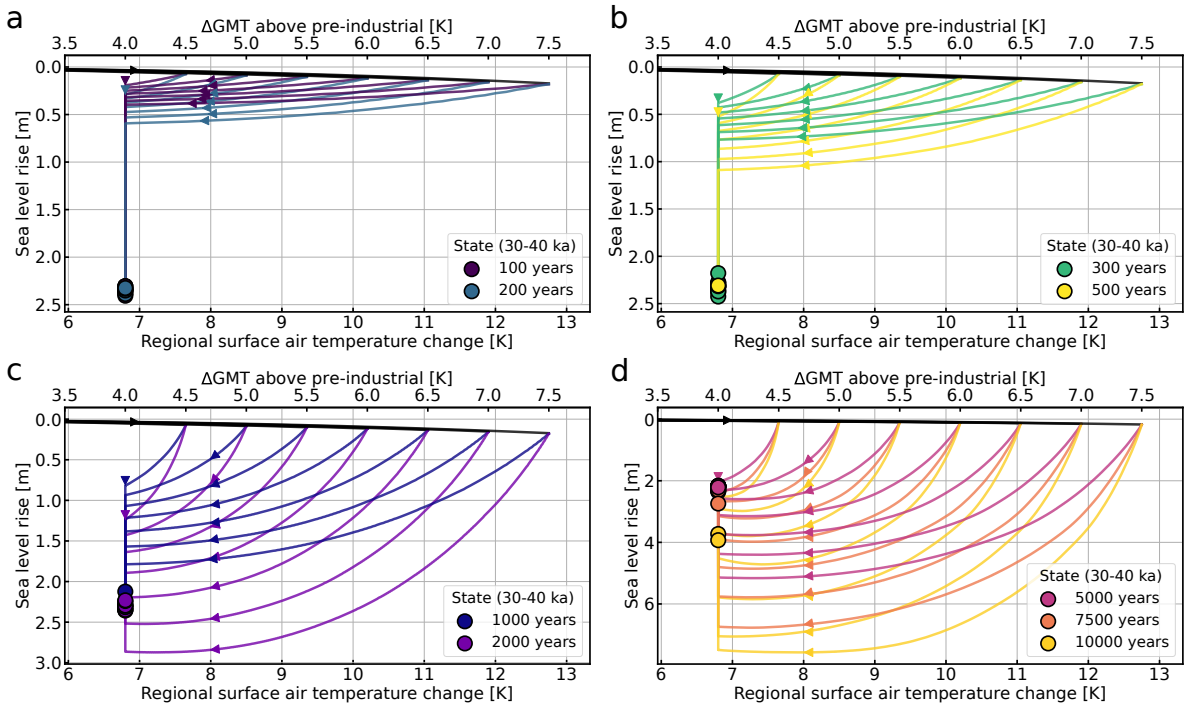

Figure S10: Trajectories of overshoot scenarios for various warming and convergence rates to 4 °C. (a) **(a)** Trajectories of ice sheet volume for various warming rates and subsequent convergence to 4.0 °C GMT above pre-industrial level for 100 and 200 years. The ice sheet recovers to a intermediate state with around 2.0-2.5 m GSLR. Longer convergence times and larger warming cause larger ice sheet loss before partial recovery. **(b)**, **(c)** and **(d)** same as **(a)** but for convergence times between 300 and 10000 years. The ice volume after 30-40 ka is significantly lower than for more moderate scenarios (Fig. S6).

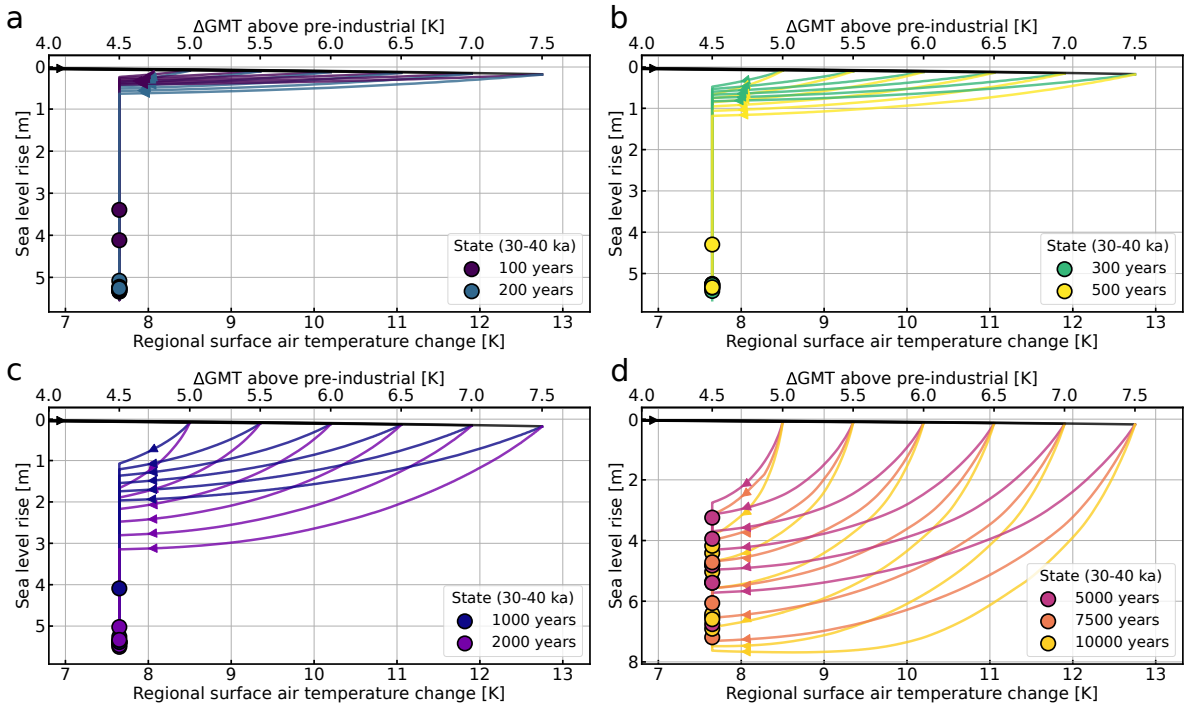

Figure S11: Trajectories of overshoot scenarios for various warming and convergence rates to 4.5 °C. (a) Trajectories of ice sheet volume for various warming rates and subsequent convergence to 4.5 °C GMT above pre-industrial level for 100 and 200 years. The ice sheet does not recover to a close to present-day configuration but an almost ice-free state with a GSLR between than 4 m and 6 m. **(b)**, **(c)** and **(d)** same as **(a)** but for convergence times between 300 and 10000 years. The ice volume after 30-40 ka is significantly lower than for more moderate scenarios (Fig. S6).

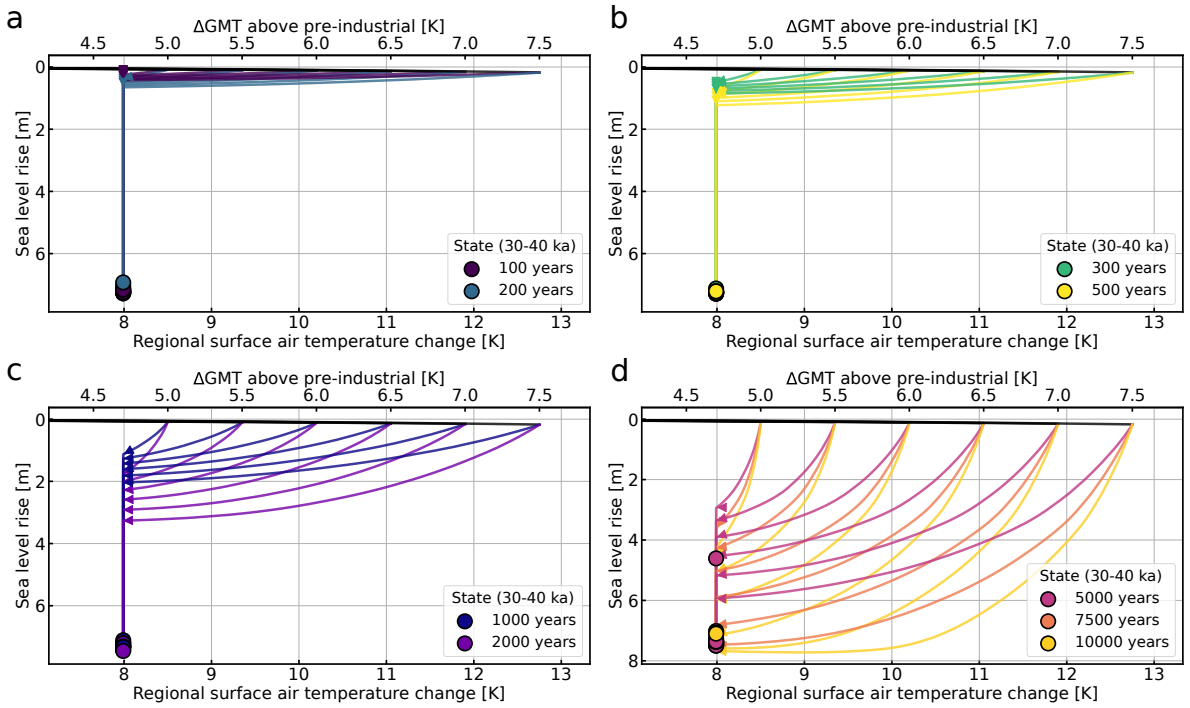

Figure S12: Trajectories of overshoot scenarios for various warming and convergence rates to 4.7 °C. (a) Trajectories of ice sheet volume for various warming rates and subsequent convergence to 4.7 °C GMT above pre-industrial level for 100 and 200 years. The ice sheet does not recover to a close to present-day configuration but an almost ice-free state with a GSLR of more than 6 m. **(b)**, **(c)** and **(d)** same as **(a)** but for convergence times between 300 and 10000 years. The ice volume after 30-40 ka is significantly lower than for more moderate scenarios (Fig. S6).

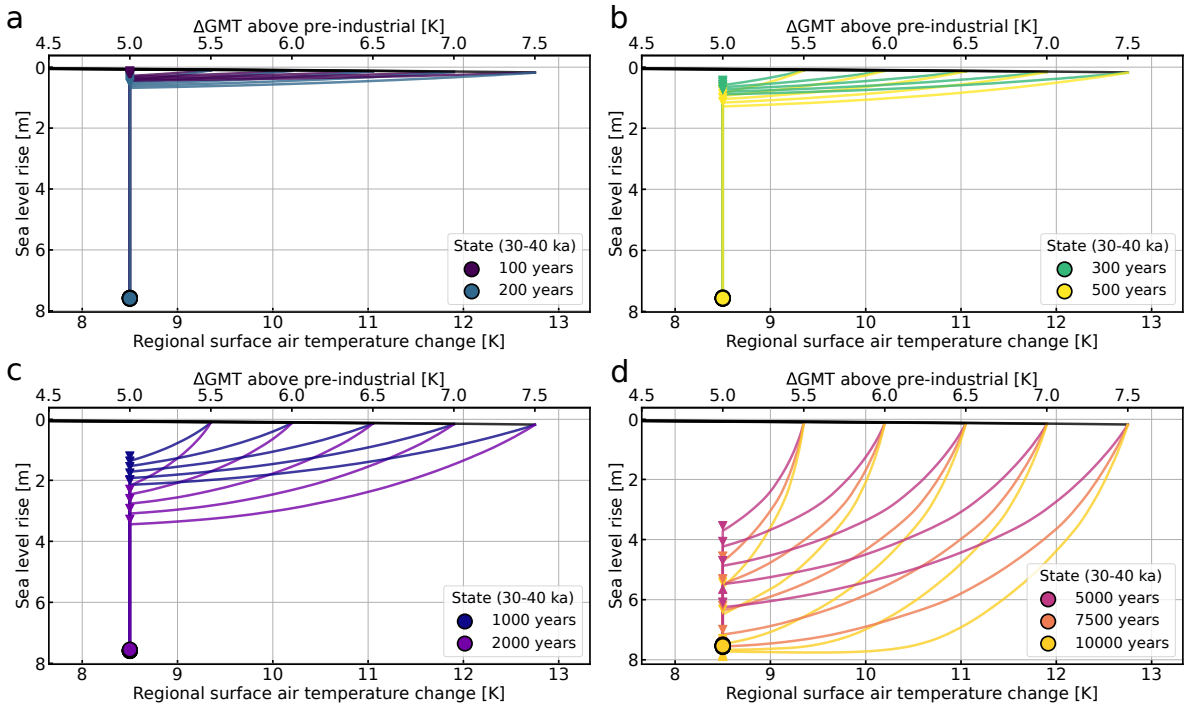

Figure S13: Trajectories of overshoot scenarios for various warming and convergence rates to 5.0 °C. (a) **(a)** Trajectories of ice sheet volume for various warming rates and subsequent convergence to 5.0 °C GMT above pre-industrial level for 100 and 200 years. The ice sheet is completely retracted with a GSLR of more than 7 m. **(b)**, **(c)** and **(d)** same as **(a)** but for convergence times between 300 and 10000 years.

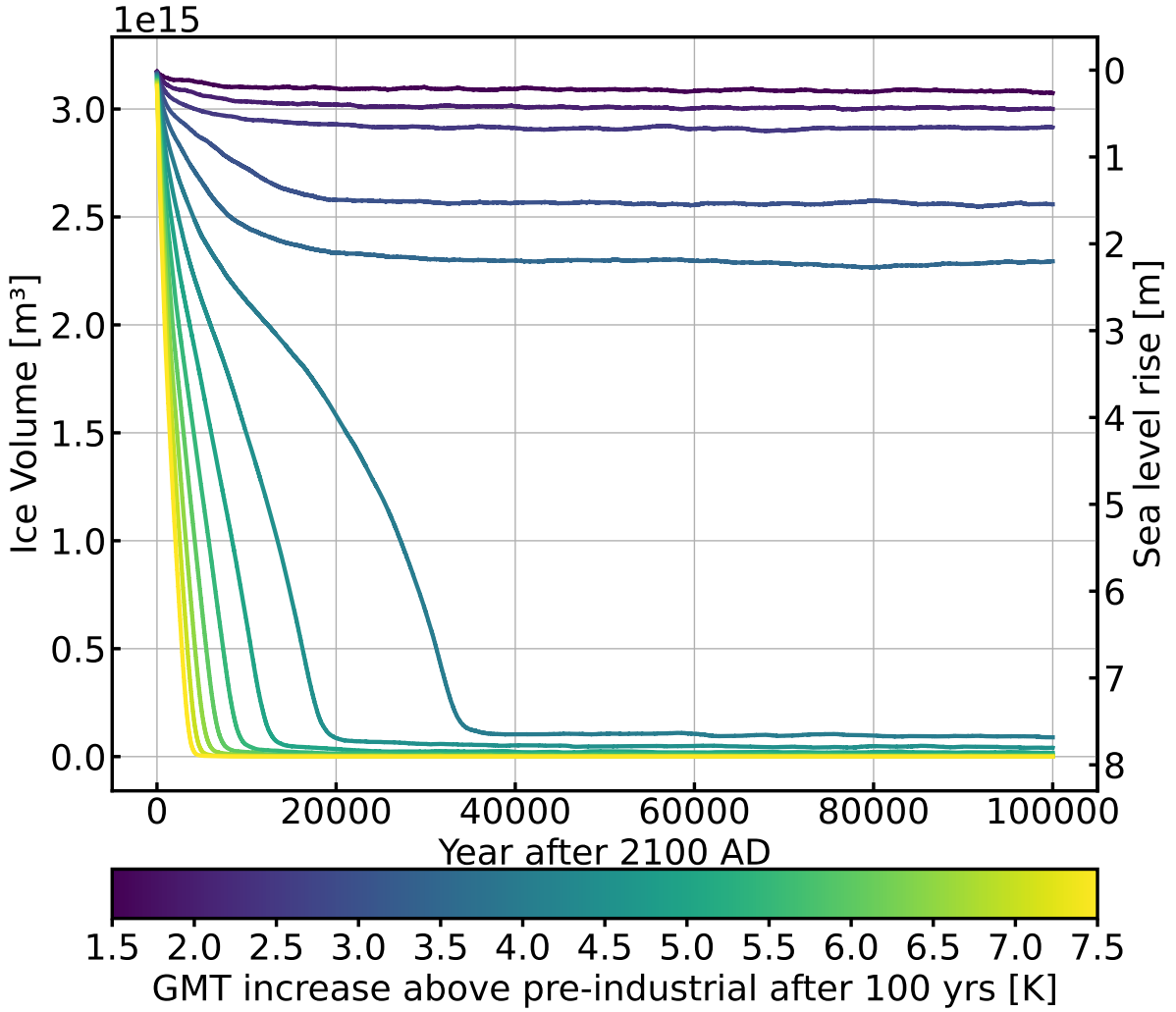

Figure S14: Time series of ice volume for different warming scenarios without glacial isostatic adjustment. Same as Fig. 1 but without glacial isostatic adjustment. Evolution of total GrIS ice volume for GMT changes between 1.5 °C and 7.5 °C above pre-industrial. The warming period lasts for 100 years (1.5 °C to 7.5 °C) and GMTs are kept constant afterwards. Three different states are noticeable: (i) present-day configuration with fully extended ice sheet, (ii) intermediate state with around 55% of present-day ice volume, and (iii) ice free state.

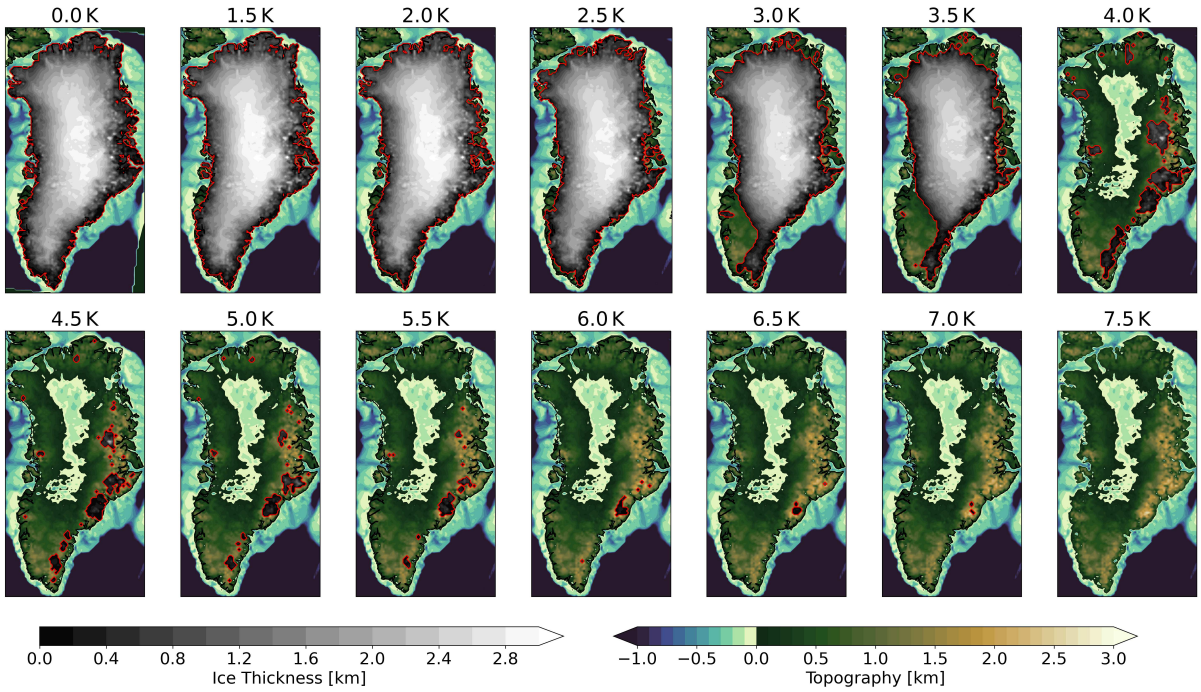

Figure S15: Spatial maps of the GrIS after 100 ka for different warming scenarios without glacial isostatic adjustment. Same figure as Fig. S2 but without glacial isostatic adjustment. Equilibrium states of the Greenland ice sheet for global warming rates between 0 °C and 7.5 °C. The warming period lasts for 100 years and the temperature is kept constant afterwards. Several different states are distinct: present-day configuration with fully extended ice sheet, several intermediate states with around 70-90% of present-day ice volume for warming rates between 0 °C and 3.5 °C, and an ice free state. The ice sheet extent is denoted by a red outline. The spatial configurations correspond to the end states in Fig. S14.

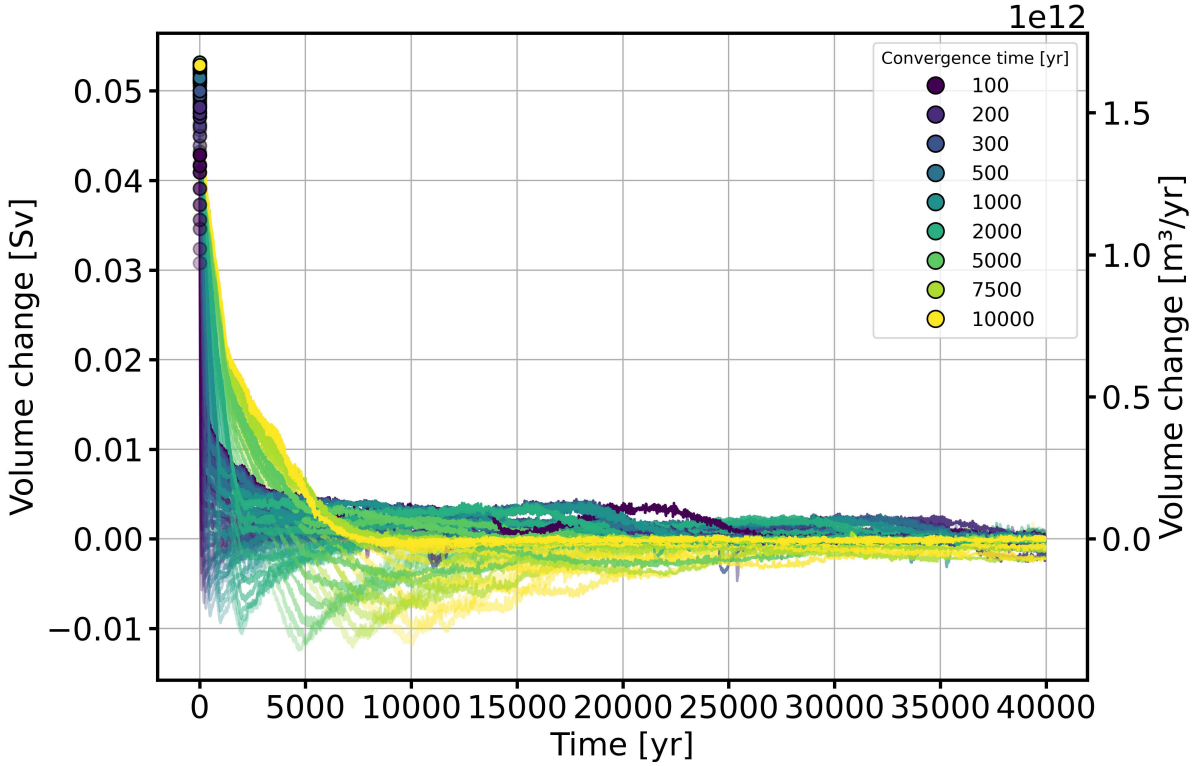

Figure S16: Volume change of GrIS for different convergence times temperatures. Time series of the volume change for maximum GMT of 7.5 °C for all considered convergence times from 100-10000 years and convergence temperatures. The alpha value corresponds to different convergence temperatures (1.5 °C (transparent) to 5 °C (opaque)). The maximum volume change for every scenario is marked as a dot. We show the rolling mean of the volume change in a sliding window of 50 years to filter out high frequency fluctuations.

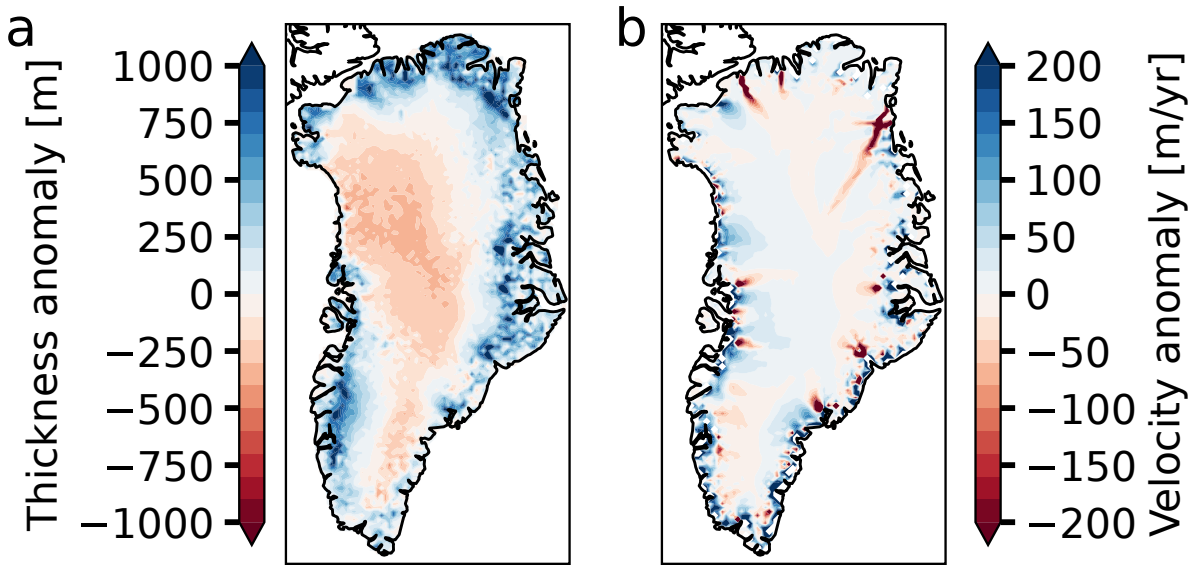

Figure S17: Difference between observed and simulated initial state ice thickness and velocity. **(a)** Difference between simulated initial state and observed ice thickness (BedMachinev5, [1, 2]). Blue areas denote regions where the simulation overestimate the thickness and red where the simulation underestimate the thickness respectively. The root mean square error is 344 m. Observational data was regridded to 20 km grid to ensure comparability. **(b)** Same as **(a)** but for the ice sheet velocity (MEaSUREsv1, [3, 4]). The root mean square error is 132 m/yr.

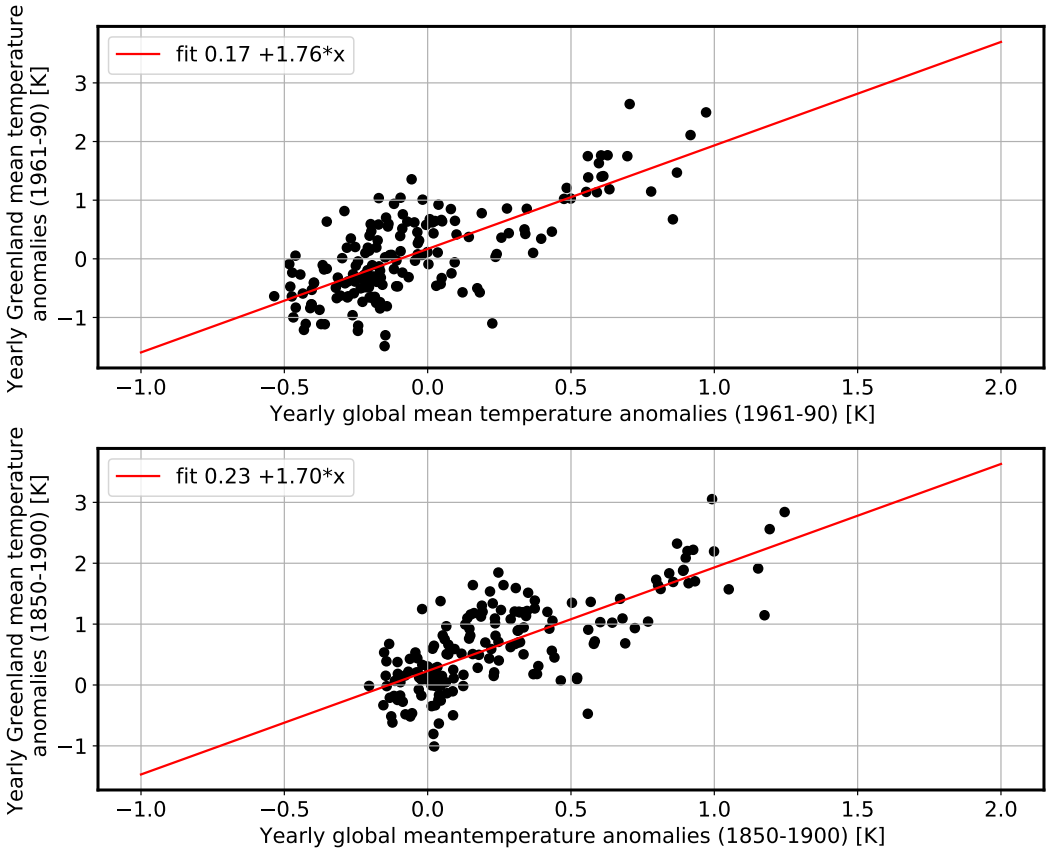

Figure S18: Fit of historical air surface temperature in Greenland against GMT. Linear fit of the yearly mean surface air temperature anomalies around Greenland against global mean surface air temperature anomalies for two different reference periods (1961-1990 and 1850-1900). The temperatures are taken from HadCRUT5 [5]. Both reference periods show a scaling factor of around 1.7 between the temperature atound Greenland and the GMT.

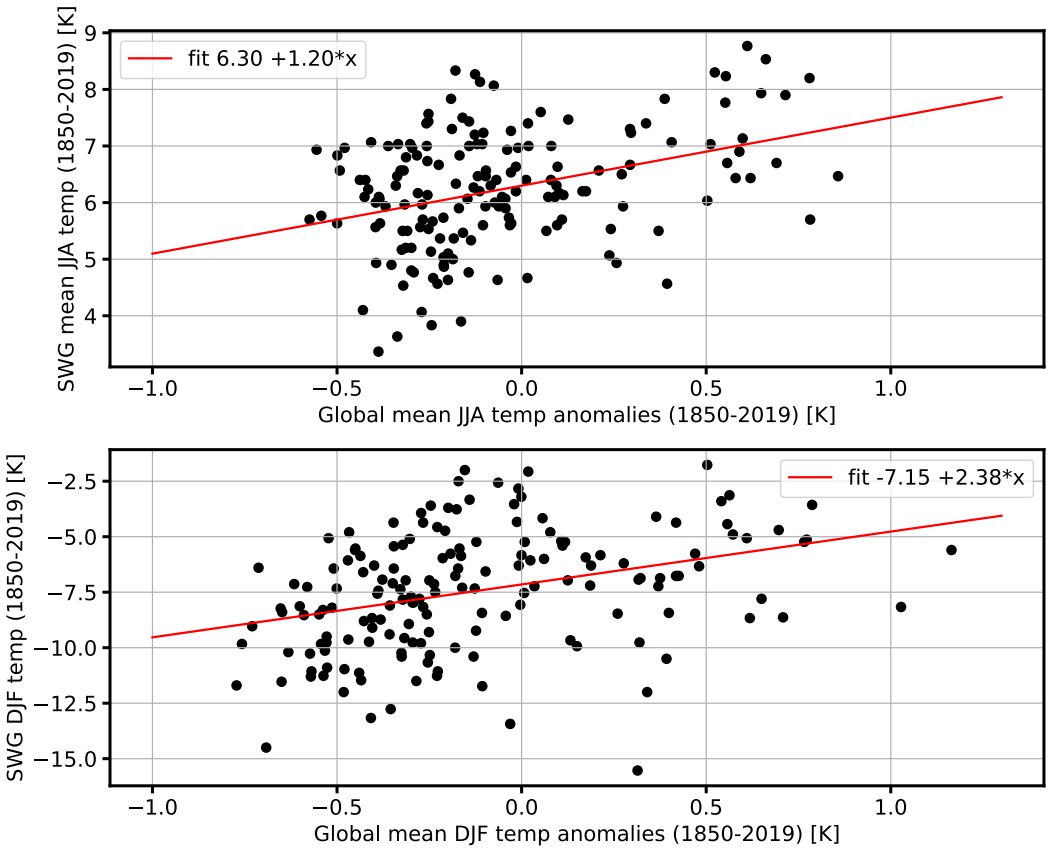

Figure S19: Fit of historical air surface temperature in southwestern Greenland against GMT. Linear fit of summer and winter mean surface air temperature in southwestern Greenland (SWG) against global mean surface air temperature anomalies in summer and winter for 1850-2019. The temperatures are taken from HadCRUT5 [5]. The scaling factors agree with the CMIP6 derived scaling factors.

Table S1: Scaling factor between global mean surface temperature and the mean surface temperature in Greenland. List of the 37 CMIP6 models [6] used for the scaling factor comparison. The second and third columns show the scaling factor between global mean surface temperature and the mean surface temperature in Greenland respectively for historical and SSP585 runs.

Model name	Historical scaling factor	SSP585 scaling factor
ACCESS-CM2	2.1157	1.5608
ACCESS-ESM1-5	2.8098	1.8150
AWI-CM-1-1-MR	1.9992	1.5575
BCC-CSM2-MR	1.9619	1.5713
CAMS-CSM1-0	1.3117	1.3528
CanESM5	1.9659	1.7299
CESM2	2.2085	1.2916
CESM2-WACCM	2.2206	1.4361
CIESM	0.8820	2.1570
CMCC-CM2-SR5	1.7970	1.9938
CMCC-ESM2	2.1475	2.1093
CNRM-CM6-1	3.2229	1.6909
CNRM-CM6-1-HR	1.7591	1.6391
CNRM-ESM2-1	2.6472	1.6088
EC-Earth3	3.3429	1.7032
EC-Earth3-CC	4.2210	1.9673
EC-Earth3-Veg	3.8206	1.8648
EC-Earth3-Veg-LR	3.9467	1.9384
FGOALS-f3-L	1.7873	1.7658
FGOALS-g3	1.3330	1.3244
FIO-ESM-2-0	1.7563	1.8711
GFDL-ESM4	1.1481	1.3143
HadGEM3-GC31-LL	1.4464	1.6969
HadGEM3-GC31-MM	1.8114	1.5282
INM-CM4-8	1.4467	1.9994
INM-CM5-0	1.7274	1.7573
IPSL-CM6A-LR	1.9993	1.7724
KIOST-ESM	1.4617	1.2714
MIROC6	1.6270	1.9729
MIROC-ES2L	1.4302	1.7184
MPI-ESM1-2-HR	1.9350	1.6315
MPI-ESM1-2-LR	1.8905	1.4931
MRI-ESM2-0	1.5220	1.3838
NESM3	2.1238	1.7064
NorESM2-LM	1.4246	1.7941
NorESM2-MM	1.7169	1.4638
UKESM1-0-LL	2.6868	1.7144
Mean	2.07	1.68
SD	0.78	0.23

Table S2: Scaling factor between global mean winter surface temperature and the mean winter surface temperature in Greenland. List of the 37 CMIP6 models [6] used for the scaling factor comparison. The second and third columns show the scaling factor between global mean winter surface temperature and the mean winter surface temperature in Greenland respectively for historical and SSP585 runs.

Model name	Historical scaling factor	SSP585 scaling factor
ACCESS-CM2	2.1108	2.0628
ACCESS-ESM1-5	3.0290	2.4893
AWI-CM-1-1-MR	2.4368	2.0893
BCC-CSM2-MR	2.3569	2.2012
CAMS-CSM1-0	1.4305	1.7077
CanESM5	2.5194	2.3319
CESM2	2.4916	1.5699
CESM2-WACCM	2.4303	1.8624
CIESM	0.8426	2.3796
CMCC-CM2-SR5	2.4836	2.4031
CMCC-ESM2	2.5761	2.6351
CNRM-CM6-1	3.3535	1.9904
CNRM-CM6-1-HR	2.3048	1.9781
CNRM-ESM2-1	2.6148	1.8726
EC-Earth3	4.1063	1.7578
EC-Earth3-CC	5.4077	2.1415
EC-Earth3-Veg	4.5076	2.0512
EC-Earth3-Veg-LR	4.9075	2.1141
FGOALS-f3-L	2.0643	2.3983
FGOALS-g3	1.0009	1.6047
FIO-ESM-2-0	1.7952	2.3380
GFDL-ESM4	1.0729	1.4608
HadGEM3-GC31-LL	1.5230	2.0670
HadGEM3-GC31-MM	2.0587	1.8166
INM-CM4-8	2.0566	2.5858
INM-CM5-0	1.6911	2.1922
IPSL-CM6A-LR	2.0000	2.1279
KIOST-ESM	1.6362	1.4998
MIROC6	2.0108	2.5869
MIROC-ES2L	1.4002	2.0772
MPI-ESM1-2-HR	2.2228	2.2028
MPI-ESM1-2-LR	2.1331	1.7292
MRI-ESM2-0	1.5811	1.8124
NESM3	2.2598	2.2720
NorESM2-LM	1.4802	2.1950
NorESM2-MM	1.2522	1.6208
UKESM1-0-LL	3.4901	2.0927
Mean	2.3416	2.0627
SD	1.0432	0.3134

Table S3: Scaling factor between global mean summer surface temperature and the mean summer surface temperature in Greenland. List of the 37 CMIP6 models [6] used for the scaling factor comparison. The second and third columns show the scaling factor between global mean summer surface temperature and the mean summer surface temperature in Greenland respectively for historical and SSP585 runs.

Model name	Historical scaling factor	SSP585 scaling factor
ACCESS-CM2	1.5007	1.0978
ACCESS-ESM1-5	1.5947	0.9949
AWI-CM-1-1-MR	1.2267	1.0196
BCC-CSM2-MR	0.9922	0.9548
CAMS-CSM1-0	0.6255	0.6664
CanESM5.r1i1p2f1	1.2261	1.0691
CESM2.r4i1p1f1	1.5785	0.9873
CESM2-WACCM	1.5105	1.0595
CIESM	0.7425	1.9601
CMCC-CM2-SR5	1.4773	1.6570
CMCC-ESM2	1.5288	1.6805
CNRM-CM6-1	2.8433	1.3488
CNRM-CM6-1-HR	1.3450	1.2339
CNRM-ESM2-1	2.5156	1.3305
EC-Earth3	2.5569	1.7250
EC-Earth3-CC	3.1429	2.0697
EC-Earth3-Veg	2.8354	1.8346
EC-Earth3-Veg-LR	3.1837	1.9871
FGOALS-f3-L	0.9342	1.0142
FGOALS-g3	1.1945	0.8743
FIO-ESM-2-0	1.4498	1.5034
GFDL-ESM4	0.8577	1.0230
HadGEM3-GC31-LL	1.2043	1.3702
HadGEM3-GC31-MM	1.4617	1.2986
INM-CM4-8	0.9112	1.0613
INM-CM5-0	1.4216	1.0372
IPSL-CM6A-LR	1.3857	1.4201
KIOST-ESM	1.0390	0.8158
MIROC6	1.2523	1.2189
MIROC-ES2L	0.7623	1.0000
MPI-ESM1-2-HR	1.3434	1.0934
MPI-ESM1-2-LR	1.3376	1.0490
MRI-ESM2-0	1.2020	0.9771
NESM3	1.6119	1.1252
NorESM2-LM	0.6723	1.2127
NorESM2-MM	1.1546	1.0089
UKESM1-0-LL	1.8658	1.3907
Mean	1.4997	1.2479
SD	0.6718	0.3451

References

1. Morlighem, M. *et al.* BedMachine v3: Complete Bed Topography and Ocean Bathymetry Mapping of Greenland From Multibeam Echo Sounding Combined With Mass Conservation. en. *Geophysical Research Letters* **44,** 11, 051–11, 061 (2017).

2. Morlighem, M. e. a. *IceBridge BedMachine Greenland, Version 5* 2022.

3. Joughin, I., Smith, B. & Howat, I. *MEaSUREs Multi-year Greenland Ice Sheet Velocity Mosaic, Version 1* 2016.

4. Joughin, I., Smith, B. E. & Howat, I. M. A complete map of Greenland ice velocity derived from satellite data collected over 20 years. en. *Journal of Glaciology* **64,** 1–11 (Feb. 2018).

5. Morice, C. P. *et al.* An Updated Assessment of Near-Surface Temperature Change From 1850: The HadCRUT5 Data Set. en. *Journal of Geophysical Research: Atmospheres* **126,** e2019JD032361 (2021).

6. Eyring, V. *et al.* Overview of the Coupled Model Intercomparison Project Phase 6 (CMIP6) experimental design and organization. English. *Geoscientific Model Development* **9,** 1937–1958 (May 2016).